

Original Research Communication

Oxygen: From the Benefits of Inducing VEGF Expression to Managing the Risk of Hyperbaric Stress

VIREN PATEL,¹ INDIRA V. CHIVUKULA,¹ SASHWATI ROY,¹ SAVITA KHANNA,¹
GUANGLONG HE,² NAVDEEP OJHA,¹ AMITA MEHROTRA,¹ LISA M. DIAS,¹
THOMAS K. HUNT,³ and CHANDAN K. SEN¹

ABSTRACT

Hypoxia limits wound healing. Both normobaric (1 atm) and hyperbaric oxygen (HBO) approaches have been used clinically to oxygenate wound tissue. Recently, we reported that HBO ameliorates stress-induced impairment of dermal healing. We examined the effect of pressure on oxygen-induced vascular endothelial growth factor (VEGF) expression by human HaCaT keratinocytes. Next, we investigated the effect of HBO on whole-body redox and on the ratio of oxidized to reduced glutathione (GSSG/GSH) in the liver, heart, lung, and brain of rats. Superoxygenation (90% O₂) of keratinocytes partially arrested cell growth. G2-M growth arrest was substantially augmented by HBO. HBO also caused apoptosis in a small subpopulation. Normobaric oxygen, but not HBO (2 atm), potently induced the expression of VEGF165 and 189. *In vivo* electron paramagnetic resonance spectroscopy imaging revealed a clear shift of the whole-body redox status toward oxidation in response to HBO. The standard diet of laboratory rats contains excessive (17× human recommended dietary allowance) α-tocopherol (E⁺⁺), which confers exceptional resistance to oxidant insults. People with chronic wounds commonly suffer from under- or malnutrition. We generated vitamin E-deficient (E⁻) rats by long-term dietary vitamin E restriction. HBO did not raise GSSG/GSH in E⁺⁺ rats, but post-HBO GSSG/GSH was significantly higher in E⁻ compared with E⁺⁺. Thus, rats on antioxidant-enriched diet were well protected against HBO. The risk of oxidative stress may negatively impact the net benefits of HBO. This is of special concern for people with inadequate intake of dietary antioxidants. Nutritional antioxidant supplementation may offset HBO-induced oxidative stress. *Antioxid. Redox Signal.* 7, 1377–1387.

INTRODUCTION

HYPOXIA, caused by disrupted vasculature, is a key factor that limits wound healing. Correcting this compromised state of tissue oxygenation by the administration of supplemental O₂ may benefit wound healing in the perioperative and outpatient setting (18). Clinical trials have shown that keeping patients warm and administering supplemental O₂, both of which enhance wound oxygenation, decrease the rate of wound infection in surgical patients and shorten the average length of hospital stay (19, 30). Beyond its role as a nutrient

and antibiotic, O₂ may support vital processes, such as angiogenesis (18). The central area of the wound is most hypoxic with a progressive increase in the O₂ gradient toward the uninjured tissue at the periphery. The *p*O₂ of dermal wounds ranges from 0–10 mm Hg centrally to 60 mm Hg at the periphery, whereas the *p*O₂ in the arterial blood is ~100 mm Hg. Clinical use of O₂ to promote wound healing began in the 1960s with administration of systemic hyperbaric O₂ (HBO) to treat wounds (24). More recently, the use of normobaric topical oxygen for the treatment of clinical problem wounds has shown encouraging results (27). Although the conditions

Laboratory of Molecular Medicine, Departments of ¹Surgery and ²Internal Medicine, Dorothy M. Davis Heart and Lung Research Institute, The Ohio State University Medical Center, Columbus, OH.

³Department of Surgery, University of California at San Francisco, CA.

(e.g., pressure, O₂ concentration, frequency and duration of administration) for systemic HBO therapy have not been optimized on the basis of randomized clinical trials, HBO is an FDA-approved therapeutic modality used in wound clinics (18). Recently, we have presented the first experimental evidence demonstrating that HBO may restore wound healing in stressed mice (16). Although HBO may serve as an effective tool to oxygenate wound tissue, it has some potential to cause oxygen toxicity as well. Oxygen toxicity has been known for centuries (6, 46). Recently, sensitive and specific molecular markers of oxygen toxicity have been identified (7, 57, 58). For example, isofurans have been identified as a sensitive marker of toxicity caused by oxygen with a purity greater than 21% (35). Although these novel techniques remain to be used to test the incidence of oxygen toxicity in patients receiving HBO, it has been established that HBO increases the levels of free radicals in the blood of humans (36). Furthermore, a higher incidence of oxygen-toxic seizures in the patient population receiving HBO therapy has been recently reported (20). These findings are consistent with findings in the laboratory indicating that HBO may be genotoxic (55). A favorable outcome in wound healing studies using subpure (19) and pure (27) O₂ under normobaric conditions warrants reassessing the merits of pressure in O₂ therapy. Among many known growth factors, vascular endothelial growth factor (VEGF) is believed to be the most prevalent, efficacious, and long-term signal that is known to stimulate angiogenesis in wounds (53). In this study, we sought to test the effect of pressure on oxygen-induced VEGF expression by human keratinocytes. Next, we investigated the effect of HBO exposure *in vivo* on oxidative stress status in vital organs.

MATERIALS AND METHODS

In Vitro Studies

Cell and cell culture. Immortalized HaCaT human keratinocytes were grown in Dulbecco's low-glucose modified Eagle's medium (Life Technologies, Gaithersburg, MD, U.S.A.) supplemented with 10% fetal bovine serum, 100 U/ml penicillin, and 100 µg/ml streptomycin. The cells were maintained in a standard culture incubator with humidified air containing 5% CO₂ at 37°C as described previously (53). In experiments determining the growth rate of HaCaT under varying ambient oxygen conditions, cells were seeded (5,000 cells per well) in four-well plates. The culture plates were maintained in one of three experimental conditions: 20% oxygen [room air (RA)], 90% oxygen at 1 atm pressure [normobaric oxygen (NBO)], and 90% oxygen at 2 atm pressure (HBO). Culture of cells under HBO conditions was made possible using the OxyCure®3000 hyperbaric incubator (OxyHeal, National City, CA, U.S.A.). Cells were counted using a Coulter particle counter (Beckman Coulter Inc., Miami, FL, U.S.A.). The first reading, interpreted as baseline, was collected 3 h after seeding. When required, cell culture media were collected for enzyme-linked immunosorbent assay (ELISA).

Cell cycle analysis. On days 3 and 7 of seeding, cells from each one of the three conditions (room air, NBO, and

HBO) were examined for cell cycle using flow cytometry (FACS Calibur, Becton Dickinson) and CellQuest software (BD Biosciences) as described previously (44).

VEGF assays. At specific time points after seeding of cells, 0.5 ml of culture medium was collected from each well. VEGF ELISA (R&D Systems Inc., Minneapolis, MN, U.S.A.) was performed as described previously (53). For mRNA analyses, RNA was isolated from cells in each condition using the Qiagen® RNeasy mini-protocol (Qiagen Inc., Valencia, CA, U.S.A.). VEGF (splice variants VEGF165 and VEGF189) and β-actin were detected by reverse transcription-polymerase chain reaction (RT-PCR) using primers as described previously (53). Samples were run on 2% agarose gel, and the images of the subsequent bands were used for densitometry. Data were normalized using β-actin as the housekeeping gene.

HPLC analysis of glutathione redox status. Reduced (GSH) and oxidized (GSSG) glutathione were detected simultaneously from HaCaT cell acid lysates using an HPLC-coulometric electrode array detector (CoulArray Detector, model 5600 with 12 channels; ESA Inc., Chelmsford, MA, U.S.A.) as described previously (53). In brief, cells were plated in 100-mm plates and 10 ml of medium to obtain 75% confluence on day 5 for each of the three experimental conditions. A pilot experiment was run to determine initial plating counts per condition that would provide 75% confluence on day 5. The seeding density for each of the three experimental conditions was as follows: 0.2 × 10⁶ cells per plate (RA), 0.45 × 10⁶ cells per plate (NBO), and 1 × 10⁶ cells per plate (HBO). Cells were harvested on day 5 following seeding. The samples were snap-frozen and stored in liquid nitrogen until HPLC assay. Sample preparation, composition of the mobile phase, and specification of the column used have been previously reported (52, 53). This system uses multiple channels set at different redox potentials. Data were collected using channels set at 600, 700, and 800 mV.

In vivo studies

Animals and supplementation protocol. Male and female rats (Sprague-Dawley, 14 weeks old; Harlan, Indianapolis, IN, U.S.A.) were divided into the following three groups: (a) E⁺⁺ group, male (*n* = 3) and female (*n* = 3) rats fed standard rat chow containing 200 nmol of α-tocopherol per gram dry weight; (b) E⁺⁺HBO group, male (*n* = 3) and female (*n* = 3) rats fed standard rat chow and exposed to HBO (pure O₂, 2 atm, 2 h, once); and (c) E⁻HBO group, male (*n* = 3) and female (*n* = 3) rats maintained on vitamin E-deficient diet (TD 88163, Harlan) for two generations (3 months) and exposed to HBO once. Rats were killed and tissues harvested after HBO exposure.

Vitamin E extraction and analysis. Vitamin E extraction from the liver and analysis were performed as described previously using an HPLC-coulometric electrode array detector (CoulArray Detector Model 5600 with 12 channels; ESA Inc.) (42, 43).

Tissue glutathione assay. Tissue GSH and GSSG were detected as described above for *in vitro* studies.

Electron paramagnetic resonance spectroscopy (EPR) imaging of whole-body redox. Mice in RA and HBO groups were anesthetized by intraperitoneal injection of ketamine (90 mg/kg of body weight) and xylazine (20 mg/kg). 3-Carbamoyl-proxyl solution (150 mg/kg of body weight) was injected into the tail vein, and the mouse was placed in a prone position in a quartz tube of 3.5-cm diameter. EPR spectra were immediately taken in body of the mouse at regular intervals of 4 min, and 16 projections were taken for each time point for two-dimensional imaging of redox status. The measurements were performed using a custom-built EPR spectrometer (22) fitted with a 750-MHz microwave power unit and a 40-mm diameter loop gap re-entrant resonator. The microwave power was set at 32 mW, and the modulation frequency was 100 kHz. Spectral acquisitions were performed using a custom-developed data acquisition software (SPEX) that was capable of automated data acquisition and recording. For construction of two-dimensional images, 16 projections were taken and the spectral data were deconvoluted using the line shape of the zero-gradient spectrum. Images were reconstructed from the deconvoluted data by filtered back projection.

Statistics

Bar and line graphs are reported as means \pm SD. Comparisons between means were tested using two-sample equal variance, two-tailed distribution *t* test. $p < 0.05$ was considered statistically significant.

RESULTS

Exposure of HaCaT keratinocytes to 90% oxygen limited cell growth. Growth was almost completely arrested in response to HBO (Fig. 1). Flow cytometry analyses revealed that oxygen arrested the cell cycle in the G2-M phase and that such arrest was substantially augmented in response to HBO. Concurrent with cell-cycle arrest in the G2-M phase, a very limited number of HaCaT cells (<1%) responded to oxygen exposure by undergoing apoptosis. Such death response was increased by over six-fold when cells were exposed to HBO. Thus, the pressure factor clearly played a major role in causing G2-M arrest and apoptosis (Fig. 2). Oxygen potentially induced VEGF expression by the keratinocytes. Higher levels of VEGF protein were detected in the cell-culture medium (Fig. 3A). PCR studies demonstrated that oxygen regulated VEGF production at the transcriptional level. The mRNA analyses of 165 and 189 forms of VEGF revealed that both forms of VEGF were equally sensitive to oxygen. Although both 165 and 189 forms of VEGF were significantly induced by NBO, ambient pressure emerged as a key determinant of that response. Exposure of HaCaT to HBO obliterated the effects of oxygen on inducible VEGF expression (Fig. 3). To test whether the detrimental effects of HBO on cell growth, survival, and angiogenic response were related to oxidative stress, cellular glutathione redox status was determined. Ex-

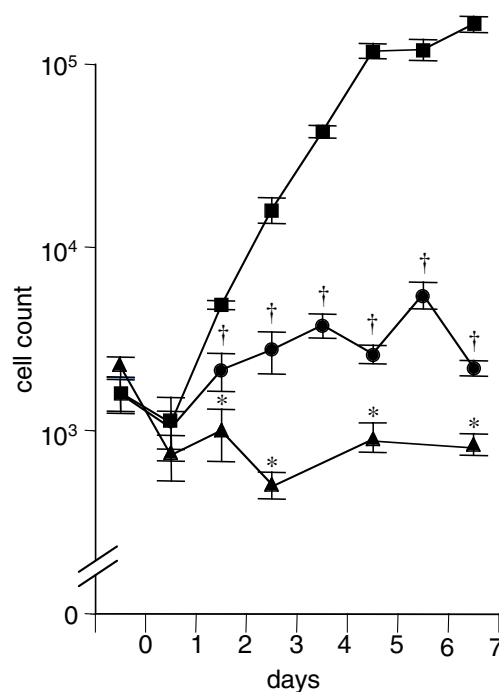


FIG. 1. Human keratinocyte cell growth in response to changes in ambient oxygen conditions. Cells (5,000 cells/well) were seeded into four-well plates. For day 0 data, attached cells were counted after 3 h of seeding. RA, ■; NBO, ●; HBO, ▲. † $p < 0.05$, significant difference between NBO and RA; * $p < 0.05$, significant difference between HBO and NBO.

posure of the cells to oxygen down-regulated cellular GSH and increased GSSG levels. This represents a shift of the cellular glutathione redox state toward oxidation. Exposure of HaCaT to HBO showed marked signs of oxidative stress as reflected by a substantial increase in cellular GSSG/GSH ratio compared with cells exposed to NBO (Fig. 4).

To verify this stressful effect of HBO *in vivo*, EPR imaging and biochemical studies were conducted. For EPR imaging, mice were chosen because our EPR cavity is suited for the size of mice. Anesthetized mice were injected with a nitroxyl radical through the tail vein and placed in the EPR resonator, and images were taken every 4 min. Antioxidants reduce the nitroxyl radical to hydroxylamine, and thus the signal decays with time. A higher intensity signal from an area indicates lower reduction capacity of the corresponding tissue. In the control group, high signal intensity was observed in the peritoneum at 4 and 8 min and in the bladder at 12 and 16 min. In the HBO group, higher signal intensity was observed at all time points as compared with the control group, and the nitroxyl radical was retained in the body for a longer time (Fig. 5). This indicates a clear shift of the whole-body redox status toward oxidation in response to HBO treatment. The EPR imaging studies thus confirmed our *in vitro* observation indicating that HBO poses the risk of oxidative stress.

Laboratory rats are fed with a standard diet that contains a substantial excess of α -tocopherol (E^{+}). Because of this, the laboratory rat is unusually enriched in antioxidants and thus

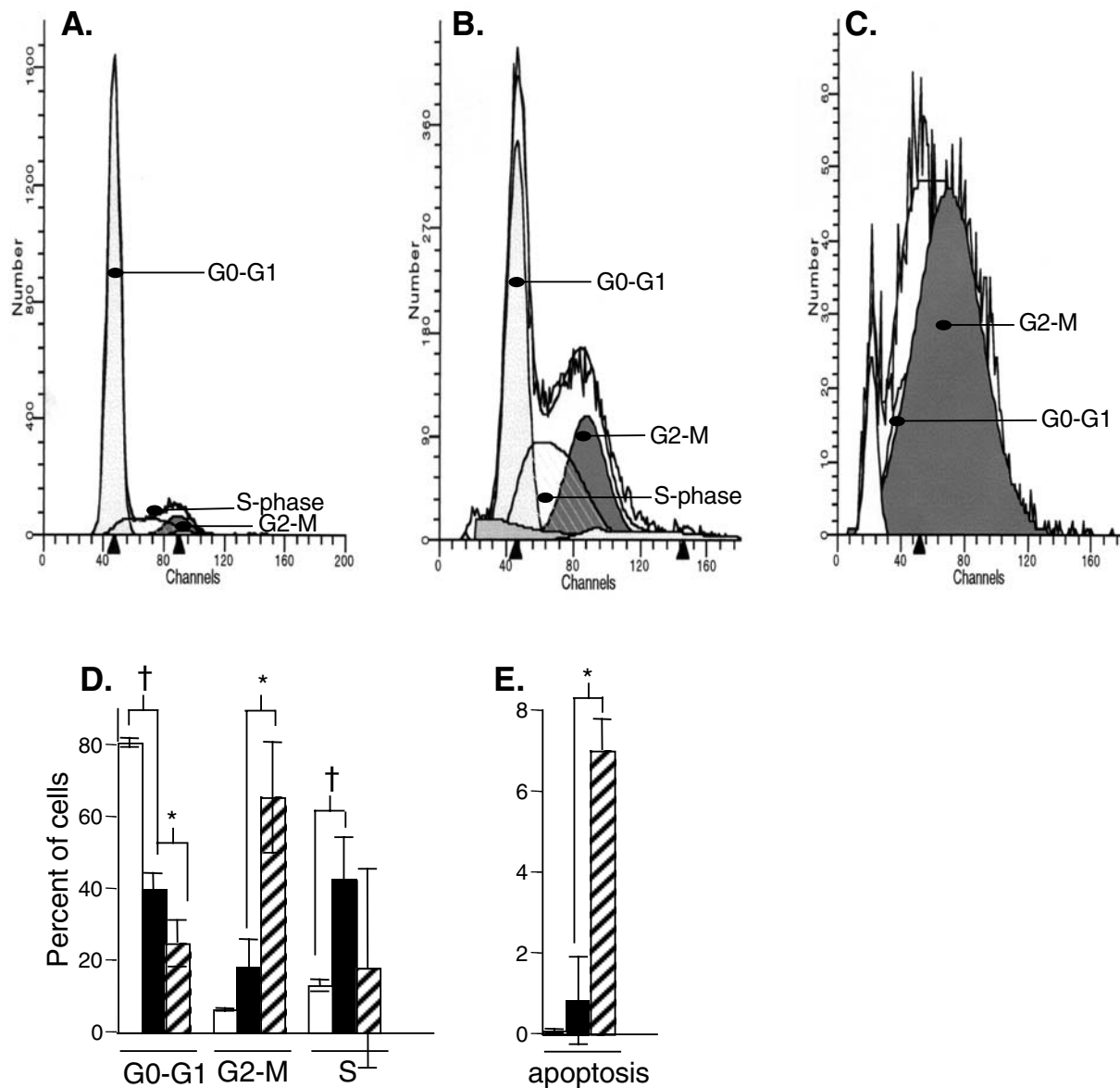


FIG. 2. Keratinocyte cell cycle in response to changes in ambient oxygen conditions. Cell cycle was analyzed on day 7 following seeding. (A) RA. (B) NBO. (C) HBO. (D and E) RA, open bar; NBO, closed bar; HBO, hatched bar. † $p < 0.05$, significant difference between RA and NBO; * $p < 0.05$, significant difference between NBO and HBO.

exceptionally resistant to oxidative stress (56). We have observed that the typical experimental rat eats 4 g of rat chow per 100 g of body weight, *i.e.*, 20 g of chow is consumed by the 500-g rat per day. The Harlan Teklad 22/5 rodent diet (W) contains 109.54 IU of dietary tocopherols per kilogram of chow. Thus, the typical 500-g adult rat ingests 2.2 IU of dietary tocopherols per day or 4.4 IU/kg of body/day. The current human recommended daily allowance (RDA) is 22.5 IU (or 15 mg; 1 mg = 1.5 IU) per day for adult men and women (25). The mean body weight for adult men in the United States during the period 1999–2002 has been determined to be 191 lb or 86.64 kg (39). Factoring in such an average body weight, the human RDA may be expressed as 0.26 IU/kg of body/day.

Thus, the standard rat chow provides 17-fold higher vitamin E to the adult laboratory rat than recommended for the average adult in the United States.

To wash off excess tissue vitamin E from laboratory rats, we maintained them on a vitamin E-deficient diet. Such dietary modulation resulted in a significant lowering of tissue vitamin E level in both male and female rats (Fig. 6). We utilized these E-deficient and E⁺⁺ rats for studies investigating the effects of HBO on the GSSG and GSH levels in vital organs. In rats fed with standard laboratory diet, females had a significantly higher hepatic α -tocopherol level than male rats. Exposure to HBO did not influence the hepatic vitamin E level (Fig. 6). Although female rats had a higher hepatic α -tocopherol level (Fig. 6),

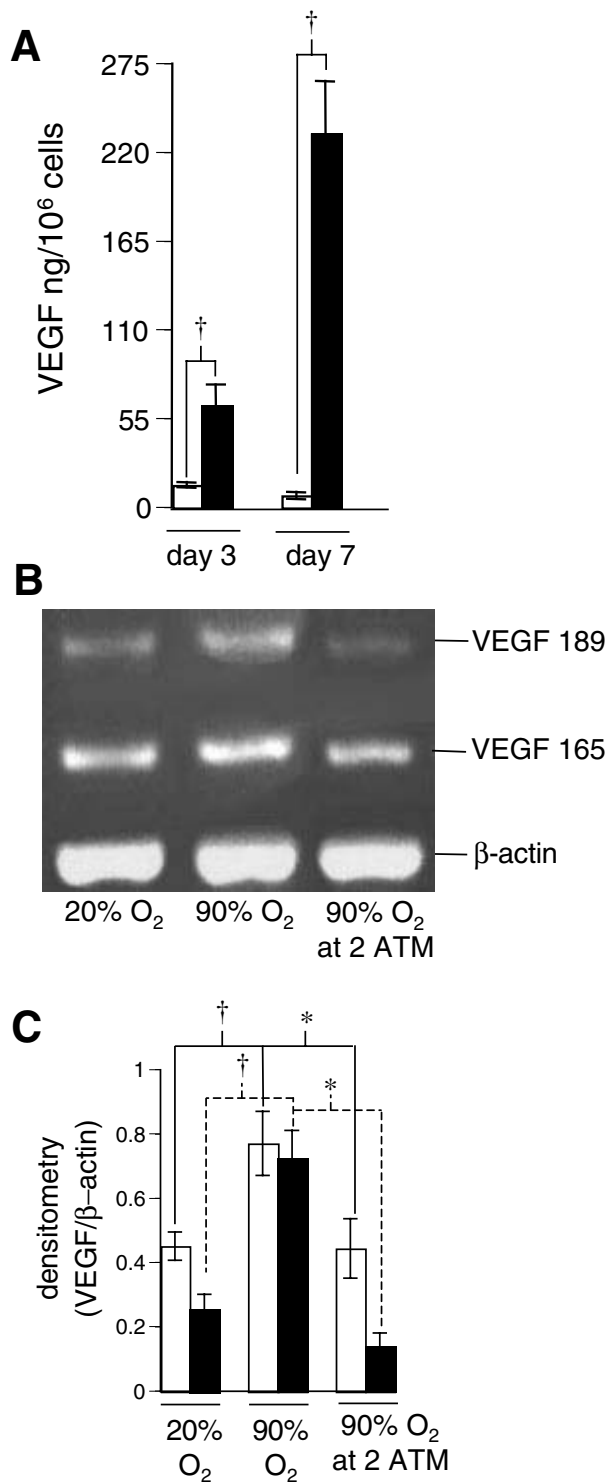


FIG. 3. Oxygen-induced VEGF expression in human keratinocytes. RA, open bar; NBO, closed bar. (A) VEGF protein in culture medium; (B) VEGF mRNA in HaCaT by RT-PCR. (C) RT-PCR densitometry data. VEGF165/β-actin, open bar; VEGF189/β-actin, closed bar. On day 3 following seeding, cells were lysed and RNA extracted for RT-PCR. †*p* < 0.05, significantly different in NBO versus RA; **p* < 0.05, significantly different in HBO versus NBO.

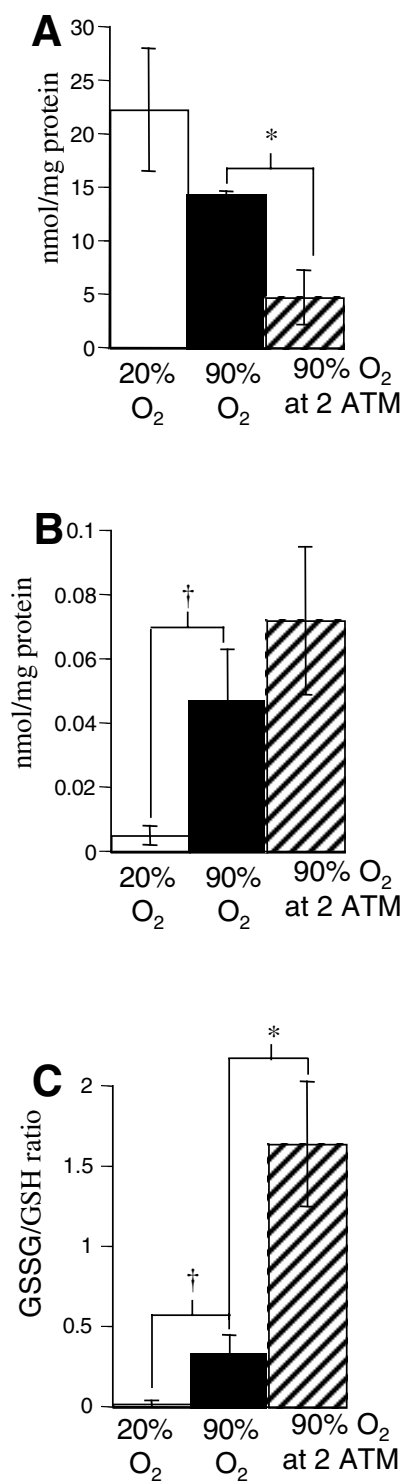


FIG. 4. Glutathione redox status in HaCaT keratinocytes in response to changes in ambient oxygen conditions. (A) GSH. (B) GSSG. (C) GSSG/GSH ratio multiplied by 100. RA, open bar; NBO, closed bar; HBO, hatched bar. Cells were plated such that on day 5, 75% confluence was achieved. Cells were harvested on day 5 of seeding. †*p* < 0.05, significantly different in NBO versus RA; **p* < 0.05, significantly different in NBO versus HBO.

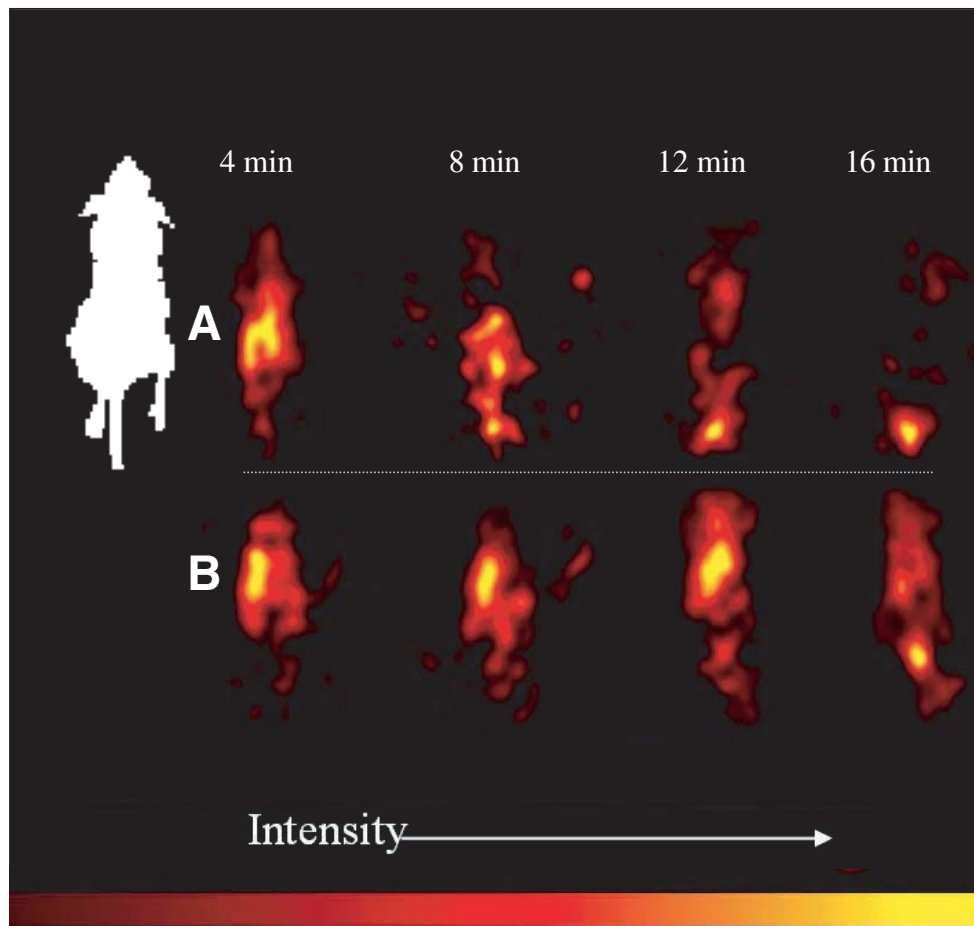


FIG. 5. Whole-body EPR redox imaging in response to HBO exposure. Tail vein injection of nitroxyl radical was followed by EPR imaging as described in Materials and Methods. Tissue antioxidants reduce the nitroxyl radical to hydroxylamine, resulting in time-dependent decay of EPR signal. A higher intensity signal from an area in the body indicates increased oxidative stress. Data were obtained using a custom-built 750-MHz EPR spectrometer with the following parameters: 32 mW microwave power, 0.7 G modulation amplitude, 100 KHz modulation frequency, 80 ms time constant, 35 G scan range, and 750 MHz microwave frequency. (**Inset**) Animal orientation. (**A**) RA control group. A high signal intensity is observed in the thoracic and peritoneal regions at 4 and 8 min after nitroxyl radical injection. This signal sharply decays with appearance of the signal in the urinary bladder as the nitroxyl probe is cleared by the kidney. (**B**) HBO-treated group. On treatment with HBO at 2 atm for 2 h once, a higher signal intensity was observed at all time points as compared with the control group, and the nitroxyl radical stayed in the body for a longer time. This observation is indicative of a shift of the tissue redox status to oxidation in response to HBO.

they had a lower hepatic GSH level than males (Fig. 7). In both males and females, a single HBO exposure tended to increase the GSSG/GSH ratio, but the effects were not significant. Post-HBO GSSG/GSH was significantly higher in male E-deficient rats (Fig. 7). In the heart, HBO did not show any effect on the tissue GSSG/GSH ratio. However, E deficiency significantly increased post-HBO GSSG/GSH in the heart of both male and female rats (Fig. 8). In the lung of male rats, HBO caused lowering of GSH. Consistent with the observation in the heart, a single exposure of HBO did not influence the lung and brain of E^{+/+} rats, but did significantly increase GSSG/GSH in E-deficient rats (Figs. 9 and 10). The HBO-exposed brain of female E-deficient rats had a higher GSSG/GSH ratio than their male counterparts (Fig. 10).

DISCUSSION

The state of tissue oxygenation is a key determinant of inducible VEGF expression and angiogenesis. Although hypoxia can initiate neovascularization by inducing angiogenic factor expression, it cannot sustain it. A threshold level of oxygenation is required to support the metabolic needs of tissue remodeling. Acutely, hypoxia facilitates the angiogenic process (45), whereas chronic hypoxia impairs wound angiogenesis (2). Sustained hypoxia causes death and dysfunction of tissue. VEGF is a major long-term angiogenic stimulus at the wound site. On the one hand, hypoxia is a potent trigger of inducible VEGF expression (5). On the other hand, hyperoxia induces VEGF as well (12, 13, 32, 54). In sum, conditions

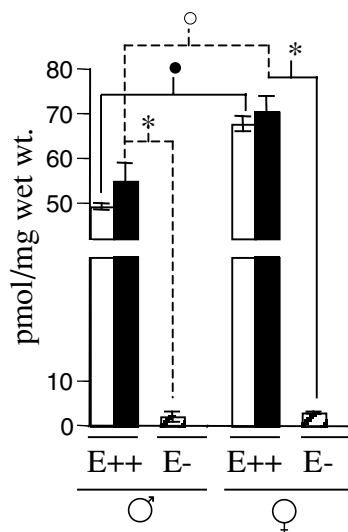


FIG. 6. Vitamin E levels in rat liver. Rats were randomly divided into the following three groups: E⁺⁺, open bar; E⁺⁺HBO, closed bar; and E⁻HBO, hatched bar. * $p < 0.05$, significant difference between E⁺⁺HBO and E⁻HBO; • $p < 0.05$, significant difference between male E⁺⁺ control and female E⁺⁺ control; ○ $p < 0.05$, significant difference between male E⁺⁺HBO and female E⁺⁺HBO. E⁺⁺ group, male ($n = 3$) and female ($n = 3$) rats fed standard chow containing 200 nmol of α -tocopherol per gram dry weight; E⁺⁺HBO group, male ($n = 3$) and female ($n = 3$) rats fed standard rat chow and exposed to HBO (pure O₂, 2 atm, 2 h, once); E⁻HBO group, male ($n = 3$) and female ($n = 3$) rats maintained on vitamin E-deficient diet for two generations (3 months) and exposed to HBO once. Rats were killed and tissues harvested after HBO exposure.

that would destabilize normoxia by either oxygen withdrawal or enrichment seem to be a trigger for inducible VEGF expression. Both hypoxia and hyperoxia are known to generate reactive oxygen species (ROS) (8, 9, 18, 48). However, ROS may induce VEGF expression independent of the hypoxia-inducible factor (53), which represents the central pathway utilized by hypoxia to regulate gene expression (31). Although the significance of the dual regulation of VEGF by oxygen remains elusive, supplemental oxygen is used clinically to support wound angiogenesis (18).

Clinical use of O₂ to promote wound healing began in the 1960s with administration of systemic HBO to treat wounds (24). Systemic HBO therapy is an FDA-approved therapeutic modality used in wound clinics with an encouraging success rate (37). However, both clinical (20) and basic science studies indicate that HBO poses the risk of oxygen toxicity. Approaches to treat wound using NBO delivery have provided beneficial outcomes in clinical settings (19, 27). Results of this study indicate that although NBO may induce VEGF expression, it causes growth arrest of <20% cells at the G2-M phase. This observation is consistent with previous findings reporting hyperoxia-induced G2-M arrest in fibroblasts (44). Of note, in a wound situation, supplemental oxygen is used to correct hypoxia and restore normoxia. Our experimental setup studied superoxygenation. Supplementation of NBO corrects hypoxia without superoxygenation (15). Thus, the growth inhibitory effects of oxygen observed in this study may not be applicable to situations where supplemental oxygen is used to correct hypoxia and not superoxygenate. The efficacy of oxygen to induce VEGF expression was completely obliterated in response to pressure. In addition, HBO completely arrested HaCaT cell growth. Previously, HBO has been observed to in-

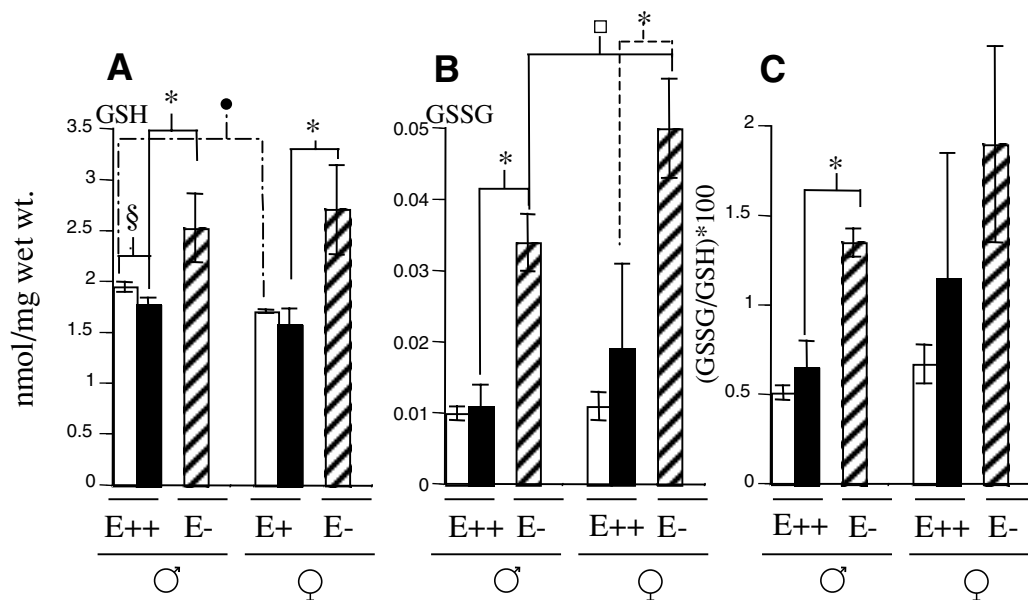
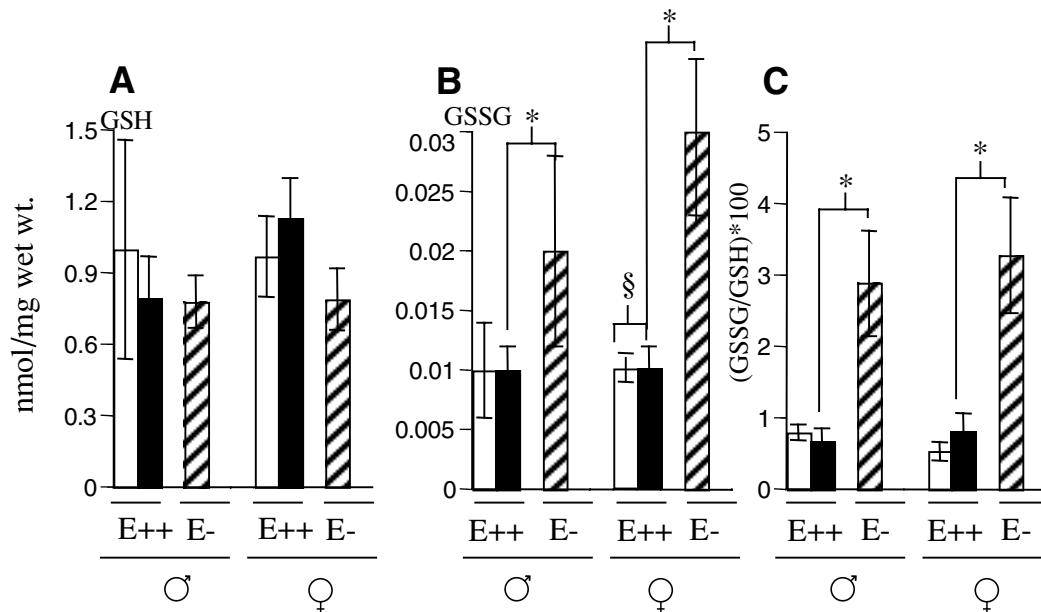


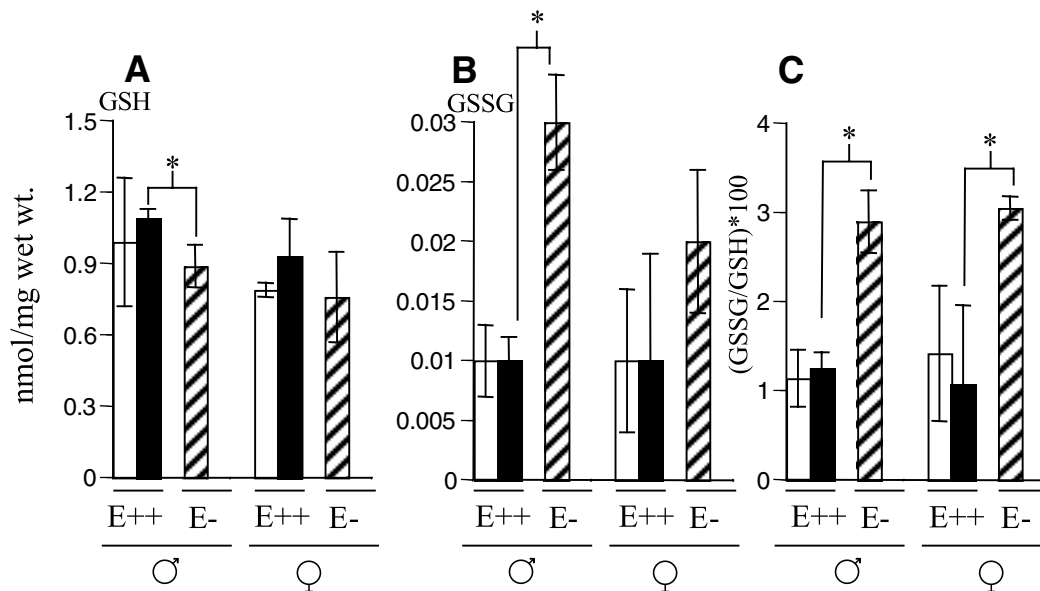
FIG. 7. Glutathione redox state levels in rat liver. * $p < 0.05$, significant difference between E⁺⁺HBO and E⁻HBO; § $p < 0.05$, significant difference between E⁺⁺ control and E⁺⁺HBO; • $p < 0.05$, significant difference between male and female E⁺⁺ control; □ $p < 0.05$, significant difference between male E⁻HBO and female E⁻HBO treated. See legend of Fig. 6 for description of groups.



hibit growth of epithelial cells (40) and induce cells to enter the cell cycle and accumulate in G2/M (28). HBO is known to superoxygenate tissues to levels multi-fold higher than their baseline pO_2 (4, 23, 38).

Both the 165 and 189 forms of VEGF were observed to be inducible by HBO. VEGF-A, the original VEGF, exists in four different isoforms (comprising 121, 165, 189, and 206 amino acids in humans), which are generated by alternative splicing of a single pre-mRNA species. The biological effects of VEGF

are mediated by two receptor tyrosine kinases, VEGFR-1 and VEGFR-2, which differ considerably in signaling properties. Nonsignaling coreceptors also modulate VEGF receptor tyrosine kinase signaling. VEGF165 and VEGF189 represent two functionally active forms of VEGF-A (3, 29). Previously, we have observed that these two specific forms of VEGF-A, but not VEGF-B, -C, or -D, are inducible by low doses of ROS (53). HBO failed to induce VEGF expression, resulted in complete growth arrest, and induced apoptosis in the keratinocytes.



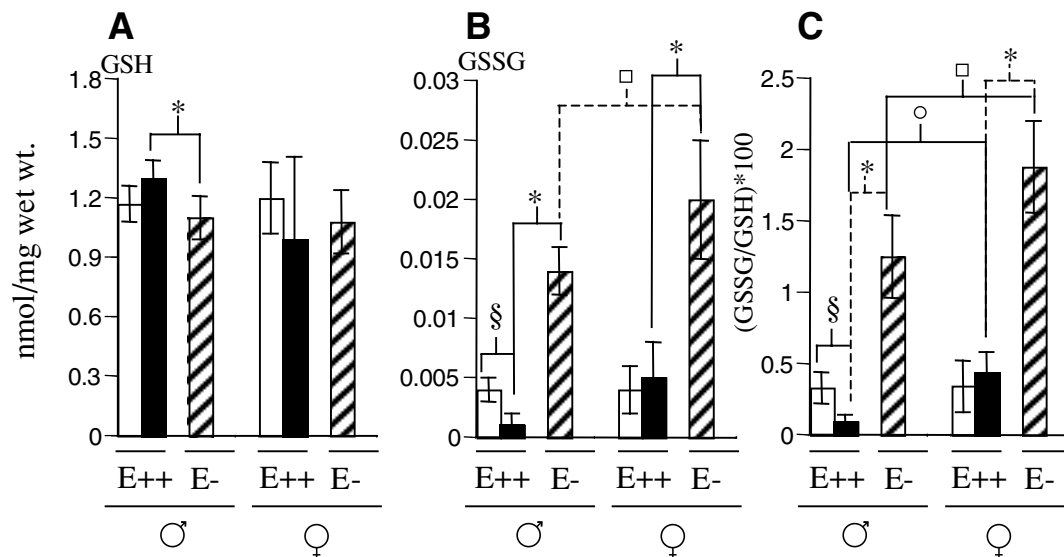


FIG. 10. Glutathione redox state levels in rat brain. * $p < 0.05$, significant difference between E⁺⁺HBO and E⁻HBO; § $p < 0.05$, significant difference between E⁺⁺ control and E⁺⁺HBO; □ $p < 0.05$, significant difference between male and female E⁻HBO; ○ $p < 0.05$, significant difference between male and female E⁺⁺HBO. See legend of Fig. 6 for description of groups.

These observations are consistent with the proapoptotic effects of HBO observed in hematopoietic cells and fibroblasts (11, 17).

In most cells, GSH is present in millimolar levels. Upon oxidant insult, GSH is rapidly oxidized to GSSG (47, 49). Thus, GSSG/GSH is used as a sensitive marker of oxidative stress (1, 50, 51). In our study, exposure of human keratinocytes to NBO elevated the GSSG/GSH ratio, indicating a tangible level of oxidant insult. This effect was increased multifold in response to HBO, indicating that pressurized oxygen caused overt oxidative stress as evidenced by growth arrest, apoptosis, and GSH oxidation. HBO is known to increase cellular free radical production (36). This is consistent with our EPR observation demonstrating a shift of the whole-body redox state toward oxidation in response to HBO treatment. Excess ROS cause GSH oxidation (26), G2/M arrest (10), and apoptosis (41). Clinically, mostly people with chronic wounds are treated with HBO. One of the most common clinical conditions associated with a nonhealing wound is compromised nutrition status (14). For example, undernutrition and malnutrition are seen at alarmingly high rates in institutionalized elderly and in patients admitted to hospitals (21). The occurrence of pressure ulcers is associated with malnutrition, as well as specific micronutrient deficiencies (33). Because laboratory rats are fed with a standard diet that contains a substantial excess of α -tocopherol (56), we decided to maintain rats on a long-term vitamin E-deficient diet in order to lower their tissue vitamin E levels to reflect the condition in malnourished or undernourished humans. We observed that HBO did not influence the GSSG/GSH ratio in the vital organs of male and female rats fed with standard laboratory chow containing excess vitamin E. This finding is in agreement with the previously reported observation that laboratory rats fed with vitamin E-enriched standard diet are exceptionally resistant to oxidative stress (56). In rats with compromised tissue vitamin E levels, however, the post-HBO GSSG/GSH ratio was significantly higher in

the E-deficient group compared with the group fed with excessive vitamin E. These findings indicate that people suffering from malnutrition or undernutrition, who are likely to have an inadequate supply of dietary vitamin E, may be sensitive to oxidative stress caused by HBO. Indeed, red blood cells in vitamin E-deficient humans are known to be adversely influenced by HBO (34).

Supplemental oxygen may support angiogenesis by a variety of mechanisms, including the induction of the biologically active forms of VEGF. Although HBO may be a useful approach to sharply raise tissue pO_2 in humans, under certain conditions it may exert adverse effects. Exposure to HBO increases the generation of oxygen free radicals in tissues, and this may be of special concern for people with inadequate intake of dietary antioxidants, such as vitamin E. Nutritional antioxidant supplementation may be considered by patients scheduled for HBO therapy. Further investigation weighing the risks and benefits of pressure in oxygen therapy is warranted.

ACKNOWLEDGMENTS

This work was supported by NIH RO1NS42617, RO1GM 69589, and RO1HL73087 to C.K.S.

ABBREVIATIONS

ELISA, enzyme-linked immunosorbent assay; EPR, electron paramagnetic resonance spectroscopy; GSH, reduced glutathione; GSSG, oxidized glutathione disulfide; HBO, hyperbaric oxygen; NBO, normobaric (1 atm) oxygen; RA, room air; RDA, recommended dietary allowance; ROS, reactive oxygen species; RT-PCR, reverse transcription-polymerase chain reaction; VEGF, vascular endothelial growth factor.

REFERENCES

- Adams JD Jr, Klaidman LK, Chang ML, and Yang J. Brain oxidative stress—analytical chemistry and thermodynamics of glutathione and NADPH. *Curr Top Med Chem* 1: 473–482, 2001.
- Allen DB, Maguire JJ, Mahdavian M, Wicke C, Marcocci L, Scheuenstuhl H, Chang M, Le AX, Hopf HW, and Hunt TK. Wound hypoxia and acidosis limit neutrophil bacterial killing mechanisms. *Arch Surg* 132: 991–996, 1997.
- Ancelin M, Buteau-Lozano H, Meduri G, Osborne-Pellegrin M, Sordello S, Plouet J, and Perrot-Applanat M. A dynamic shift of VEGF isoforms with a transient and selective progesterone-induced expression of VEGF189 regulates angiogenesis and vascular permeability in human uterus. *Proc Natl Acad Sci U S A* 99: 6023–6028, 2002.
- Becker A, Kuhnt T, Liedtke H, Krivokuca A, Bloching M, and Dunst J. Oxygenation measurements in head and neck cancers during hyperbaric oxygenation. *Strahlenther Onkol* 178: 105–108, 2002.
- Berra E, Pages G, and Pouyssegur J. MAP kinases and hypoxia in the control of VEGF expression. *Cancer Metastasis Rev* 19: 139–145, 2000.
- Bert P. *La Pression Barometrique. English Translation in 1943 by M. Hitchcock and A. Hitchcock*. Columbus, OH: College Book Company, 1978.
- Carpagnano GE, Kharitonov SA, Resta O, Foschino-Barbaro MP, Gramiccioni E, and Barnes PJ. 8-Isoprostane, a marker of oxidative stress, is increased in exhaled breath condensate of patients with obstructive sleep apnea after night and is reduced by continuous positive airway pressure therapy. *Chest* 124: 1386–1392, 2003.
- Chandel NS, Maltepe E, Goldwasser E, Mathieu CE, Simon MC, and Schumacker PT. Mitochondrial reactive oxygen species trigger hypoxia-induced transcription. *Proc Natl Acad Sci U S A* 95: 11715–11720, 1998.
- Chandel NS, McClintock DS, Feliciano CE, Wood TM, Melendez JA, Rodriguez AM, and Schumacker PT. Reactive oxygen species generated at mitochondrial complex III stabilize hypoxia-inducible factor-1 α during hypoxia: a mechanism of O₂ sensing. *J Biol Chem* 275: 25130–25138, 2000.
- Chung YW, Jeong DW, Won JY, Choi EJ, Choi YH, and Kim IY. H₂O₂-induced AP-1 activation and its effect on p21^{WAF1/CIP1}-mediated G2/M arrest in a p53-deficient human lung cancer cell. *Biochem Biophys Res Commun* 293: 1248–1253, 2002.
- Conconi MT, Baiguera S, Guidolin D, Furlan C, Menti AM, Vigolo S, Belloni AS, Parnigotto PP, and Nussdorfer GG. Effects of hyperbaric oxygen on proliferative and apoptotic activities and reactive oxygen species generation in mouse fibroblast 3T3/J2 cell line. *J Invest Med* 51: 227–232, 2003.
- Darrington RS, Godden DJ, Park MS, Ralston SH, and Wallace HM. The effect of hyperoxia on expression of cytokine mRNA in endothelial cells. *Biochem Soc Trans* 25: 292S, 1997.
- Deaton P, McKellar C, Culbreth R, Veal C, and Cooper J. Hyperoxia stimulates interleukin-8 release from alveolar macrophages and U937 cells: attenuation by dexamethasone. *Am J Physiol* 267: L187–L192, 1994.
- Farreras N, Artigas V, Cardona D, Rius X, Trias M, and Gonzalez JA. Effect of early postoperative enteral immunonutrition on wound healing in patients undergoing surgery for gastric cancer. *Clin Nutr* 24: 55–65, 2005.
- Fries RB, Wallace WA, Roy S, Kuppusamy P, Bergdall V, Gordillo GM, Melvin WS, and Sen CK. Dermal excisional wound healing in pigs following treatment with topically applied pure oxygen. *Mutat Res* (in press), 2005.
- Gajendrareddy PK, Sen CK, Horan MP, and Marucha PT. Hyperbaric oxygen therapy ameliorates stress-impaired dermal wound healing. *Brain Behav Immun* 19: 217–222, 2005.
- Ganguly BJ, Tonomura N, Benson RM, Osborne BA, and Granowitz EV. Hyperbaric oxygen enhances apoptosis in hematopoietic cells. *Apoptosis* 7: 499–510, 2002.
- Gordillo GM and Sen CK. Revisiting the essential role of oxygen in wound healing. *Am J Surg* 186: 259–263, 2003.
- Greif R, Akca O, Horn EP, Kurz A, and Sessler DI. Supplemental perioperative oxygen to reduce the incidence of surgical-wound infection. Outcomes Research Group. [See comment.] *N Engl J Med* 342: 161–167, 2000.
- Hampson N and Atik D. Central nervous system oxygen toxicity during routine hyperbaric oxygen therapy. [See comment.] *Undersea Hyperb Med* 30: 147–153, 2003.
- Harris CL and Fraser C. Malnutrition in the institutionalized elderly: the effects on wound healing. *Ostomy Wound Manage* 50: 54–63, 2004.
- He G, Petryakov S, Samouilov A, Chzhan M, Kuppusamy P, and Zweier J. Development of a resonator with automatic tuning and coupling capability to minimize sample motion noise for in vivo EPR spectroscopy. *J Magn Reson* 149: 218–227, 2001.
- Huch A, Huch R, Hollmann G, Hockerts T, Keller HP, Seiler D, Sadzek J, and Lubbers DW. Transcutaneous pO₂ of volunteers during hyperbaric oxygenation. *Biotelemetry* 4: 88–100, 1977.
- Hunt TK, Ellison EC, and Sen CK. Oxygen: at the foundation of wound healing—introduction. *World J Surg* 28: 291–293, 2004.
- Institute of Medicine FaNB. *Dietary Reference Intakes: Vitamin C, Vitamin E, Selenium, and Carotenoids*. Washington DC: National Academy Press, 2000.
- Jones CM, Lawrence A, Wardman P, and Burkitt MJ. Electron paramagnetic resonance spin trapping investigation into the kinetics of glutathione oxidation by the superoxide radical: re-evaluation of the rate constant. *Free Radic Biol Med* 32: 982–990, 2002.
- Kalliainen L, Gordillo GM, Schlanger R, and Sen CK. Topical oxygen as an adjunct to wound healing: a clinical case series. *Pathophysiology* 9: 81–87, 2003.
- Kalns JE and Piepmeier EH. Exposure to hyperbaric oxygen induces cell cycle perturbation in prostate cancer cells. *In Vitro Cell Dev Biol Anim* 35: 98–101, 1999.
- Khan A, Ashrafpour H, Huang N, Neligan PC, Kontos C, Zhong A, Forrest CR, and Pang CY. Acute local subcutaneous VEGF165 injection for augmentation of skin flap viability: efficacy and mechanism. *Am J Physiol Regul Integr Comp Physiol* 287: R1219–R1229, 2004.
- Kurz A, Sessler D, and Lenhardt R. Perioperative normothermia to reduce the incidence of surgical-wound infection and shorten hospitalization. Study of Wound Infection and Temperature Group. *N Engl J Med* 334: 1209–1215, 1996.

31. Lee JW, Bae SH, Jeong JW, Kim SH, and Kim KW. Hypoxia-inducible factor (HIF-1)alpha: its protein stability and biological functions. *Exp Mol Med* 36: 1–12, 2004.
32. Maniscalco WM, Watkins RH, Finkelstein JN, and Campbell MH. Vascular endothelial growth factor mRNA increases in alveolar epithelial cells during recovery from oxygen injury. *Am J Respir Cell Mol Biol* 13: 377–386, 1995.
33. Mechanick JI. Practical aspects of nutritional support for wound-healing patients. *Am J Surg* 188: 52–56, 2004.
34. Mengel CE. The effects of hyperoxia on red cells as related to tocopherol deficiency. *Ann NY Acad Sci* 203: 163–171, 1972.
35. Morrow JD. Introduction for special forum issue on isoprostanes and related compounds. *Antioxid Redox Signal* 7: 153–156, 2005.
36. Narkowicz CK, Vial JH, and McCartney PW. Hyperbaric oxygen therapy increases free radical levels in the blood of humans. *Free Radic Res Commun* 19: 71–80, 1993.
37. Niinikoski JH. Clinical hyperbaric oxygen therapy, wound perfusion, and transcutaneous oximetry. *World J Surg* 28: 307–311, 2004.
38. Niklas A, Brock D, Schober R, Schulz A, and Schneider D. Continuous measurements of cerebral tissue oxygen pressure during hyperbaric oxygenation—HBO effects on brain edema and necrosis after severe brain trauma in rabbits. *J Neurol Sci* 219: 77–82, 2004.
39. Ogden CL, Fryar CD, Carroll MD, and Flegal KM. Mean body weight, height, and body mass index, United States 1960–2002. *Adv Data* 1–17, 2004.
40. Padgaonkar V, Giblin FJ, Reddan JR, and Dziedzic DC. Hyperbaric oxygen inhibits the growth of cultured rabbit lens epithelial cells without affecting glutathione level. *Exp Eye Res* 56: 443–452, 1993.
41. Raha S and Robinson BH. Mitochondria, oxygen free radicals, and apoptosis. *Am J Med Genet* 106: 62–70, 2001.
42. Roy S, Lado BH, Khanna S, and Sen CK. Vitamin E sensitive genes in the developing rat fetal brain: a high-density oligonucleotide microarray analysis. *FEBS Lett* 530: 17–23, 2002.
43. Roy S, Venojarvi M, Khanna S, and Sen CK. Simultaneous detection of tocopherols and tocotrienols in biological samples using HPLC-coulometric electrode array. *Methods Enzymol* 352: 326–332, 2002.
44. Roy S, Khanna S, Bickerstaff A, Subramanian SV, Atalay M, Bierl M, Pendyala S, Levy D, Sharma N, Venojarvi M, Strauch AR, Orosz CG, and Sen CK. Oxygen sensing by primary cardiac fibroblasts: a key role of p21Waf1/Cip1/Sdi1. *Circul Res* 92: 264–271, 2003.
45. Semenza GL. HIF-1: using two hands to flip the angiogenic switch. *Cancer Metastasis Rev* 19: 59–65, 2000.
46. Sen CK. Oxygen toxicity and antioxidants: state of the art. *Indian J Physiol Pharmacol* 39: 177–196, 1995.
47. Sen CK. Nutritional biochemistry of cellular glutathione. *J Nutr Biochem* 8: 660–672, 1997.
48. Sen CK. The general case for redox control of wound repair. *Wound Repair Regen* 11: 431–438, 2003.
49. Sen CK and Packer L. Thiol homeostasis and supplements in physical exercise. *Am J Clin Nutr* 72: 653S–669S, 2000.
50. Sen CK, Atalay M, and Hanninen O. Exercise-induced oxidative stress: glutathione supplementation and deficiency. *J Appl Physiol* 77: 2177–2187, 1994.
51. Sen CK, Rankinen T, Vaisanen S, and Rauramaa R. Oxidative stress after human exercise: effect of N-acetylcysteine supplementation. [erratum appears in *J Appl Physiol* 77: following v, 1994]. *J Appl Physiol* 76: 2570–2577, 1994.
52. Sen CK, Khanna S, Roy S, and Packer L. Molecular basis of vitamin E action. Tocotrienol potently inhibits glutamate-induced pp60(c-Src) kinase activation and death of HT4 neuronal cells. *J Biol Chem* 275: 13049–13055, 2000.
53. Sen CK, Khanna S, Babior BM, Hunt TK, Ellison EC, and Roy S. Oxidant-induced vascular endothelial growth factor expression in human keratinocytes and cutaneous wound healing. *J Biol Chem* 277: 33284–33290, 2002.
54. Sheikh A, Gibson J, Rollins M, Hopf H, Hussain Z, and Hunt T. Effect of hyperoxia on vascular endothelial growth factor levels in a wound model. *Arch Surg* 153: 1293–1297, 2000.
55. Speit G, Dennog C, Radermacher P, and Rothfuss A. Genotoxicity of hyperbaric oxygen. *Mutat Res* 512: 111–119, 2002.
56. van der Worp HB, Bar PR, Kappelle LJ, and de Wildt DJ. Dietary vitamin E levels affect outcome of permanent focal cerebral ischemia in rats. *Stroke* 29: 1002–1005; discussion 1005–1006, 1998.
57. Winterbourn CC, Bonham MJ, Buss H, Abu-Zidan FM, and Windsor JA. Elevated protein carbonyls as plasma markers of oxidative stress in acute pancreatitis. *Pancreatology* 3: 375–382, 2003.
58. Wu LL, Chiou CC, Chang PY, and Wu JT. Urinary 8-OHdG: a marker of oxidative stress to DNA and a risk factor for cancer, atherosclerosis and diabetics. *Clin Chim Acta* 339: 1–9, 2004.

Address reprint requests to:
Prof. Chandan K. Sen, Ph.D.
512 Davis Heart and Lung Research Institute
The Ohio State University Medical Center
473 W. 12th Avenue
Columbus, OH 43210

E-mail: sen-1@medctr.osu.edu

Received for publication February 21, 2005; accepted April 20, 2005.